NTU GICE
Newsletter
Graduate Institute of Communication Engineering, National Taiwan University

Vol. 12, No. 4 NOV. 2021 http://www.comm.ntu.edu.tw gicenewsletter@ntu.edu.tw

In this issue

Technology Developed in GICE

CMOS Power Amplifiers for 5G mmW Applications

from Electromagnetics Group

INTRODUCTION

Several millimeter-wave (mmW) bands around 24, 28, and 39 GHz have been released for the 5G mmW communication applications. The phased array and massive MIMO technologies in 5G mmW systems usually come with multiple power amplifiers (PAs), resulting in a thermal problem. PA with high efficiency becomes an attractive research topic. PAs with enhanced efficiency has been demonstrated with class-F and inverse class-F (class-F^{-1}) topologies. By enabling non-overlapped zero-voltage switching or zero-current switching, which contributes zero power to the harmonics, the ideal 100% drain efficiency can be achieved [1]. We developed two class-F PAs in the low-cost 90-nm CMOS process. One is continuous class-F (CCF) PA for the 28 GHz band, and the other is a dual-band class-F PA for the 28 and 38 GHz bands.

CMOS Continuous Class-F PA [2]

Fig. 1 shows the schematic and chip photo of the CCF PA, a 2-stage PA implemented in the 90-nm CMOS process. The series resonator, L_2-C_2, as shown in Fig. 1, is designed to approach the 2nd harmonic frequency ($2f_o$). Hence this resonator is equivalent to a capacitor at f_o. Thus, the proposed CCF harmonic-tuned output matching network can be simplified, as shown in Fig. 2(a). This simplified circuit can provide desired optimal impedance for the PA operating at maximum output power and the reactance part of $Z_{CCF,diff}$ changes from positive to negative around 28 GHz, as shown in Fig. 3(a). Fig. 2(b) shows the equivalent half circuit of $2f_o$. In order to short out L_{cm} and form a series resonance of L_{p1}-L_2-C_2 to produce a low impedance, the resonate frequency of the L_2-C_2 series resonator is designed to be slightly higher than $2f_o$. When the frequency is changed from lower than $2f_o$ to higher

(Continued on page 2)

GICE Honors

Prof. Hsi-Tseng Chou
2021 IET Achievement Medals--Winners in Communications Engineering

Prof. Hung-yi Lee
2021 Ten Outstanding Young Taiwanese

Message from the Director

Hsi-Tseng Chou

Professor & GICE Director

This Newsletter issue reports several interesting topics. We invite Prof. Kun-You Lin and Prof. Ai-Chun Pang to share their recent research. Please grab a coffee or tea and enjoy reading their research works.

Also, we have great news to share. Recently, there are several professors and students from GICE received different awards. If you are interested in, you can take a look on the GICE website. Congratulations to them!

May the coming New Year bring you joy, love and peace. It's getting colder, please wear warm and take care!

Technology *(Continued from page 1)*

than $2f_o$, the behavior of the L_{p1}-L_2-C_2 series resonator will be transformed from capacitive into inductive. Thus, the reactance part of $Z_{CCF,com}$ is changing from negative to positive around 56 GHz, as shown in Fig. 3(b). Fig. 2(c) shows the equivalent half circuit of 3rd harmonic frequency ($3f_o$). Both of the transformer and the series resonator, L_2-C_2, behave like a small inductor at $3f_o$. Therefore, a parallel resonator consisting of the transformer, L_2-C_2, L_{p1}, and C_{ds} can produce a high impedance, as shown in Fig. 3(c). According to the frequency response of the imaginary part of f_o, $2f_o$, and $3f_o$, the proposed CCF output matching network satisfies the required impedance conditions of CCF PA.

Fig. 4(a) shows the simulated and measured gain, output power, and PAE at 27 GHz. The PA achieves the gain of 26 dB, peak PAE of 32%, P_{sat} of 15.5 dBm, and OP_{1dB} of 13.7 dBm. The PAE at the OP_{1dB} is 25.7%. The simulated and measured P_{sat} and peak PAE from 26 GHz to 32 GHz are presented in Fig. 4(b). The 1-dB bandwidth of P_{sat} is from 27 to 31 GHz, and the peak PAE is higher than 20% from 26 to 31 GHz.

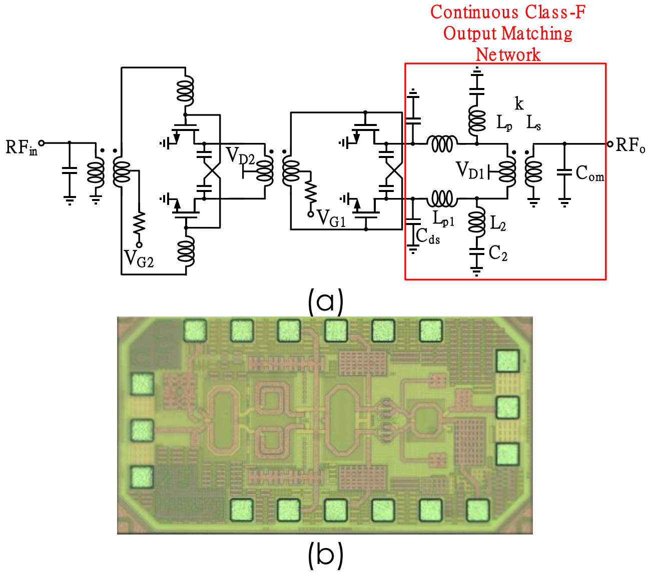

Fig. 1. (a) Schematic, and (b) chip photo of the CMOS CCF PA.

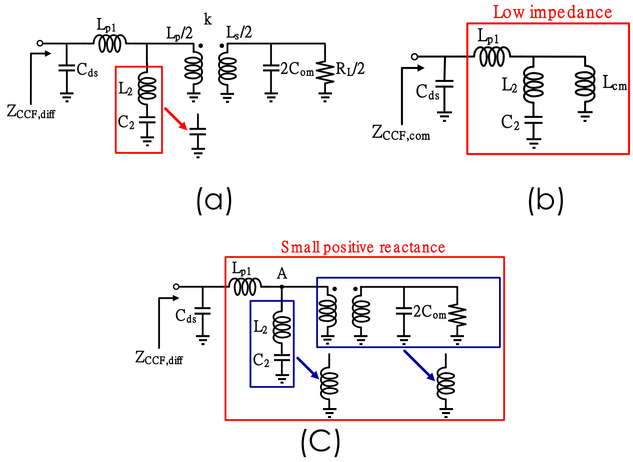

Fig. 2 Equivalent half circuits of proposed CCF output matching network at (a) f_o, (b) $2f_o$, and (c) $3f_o$.

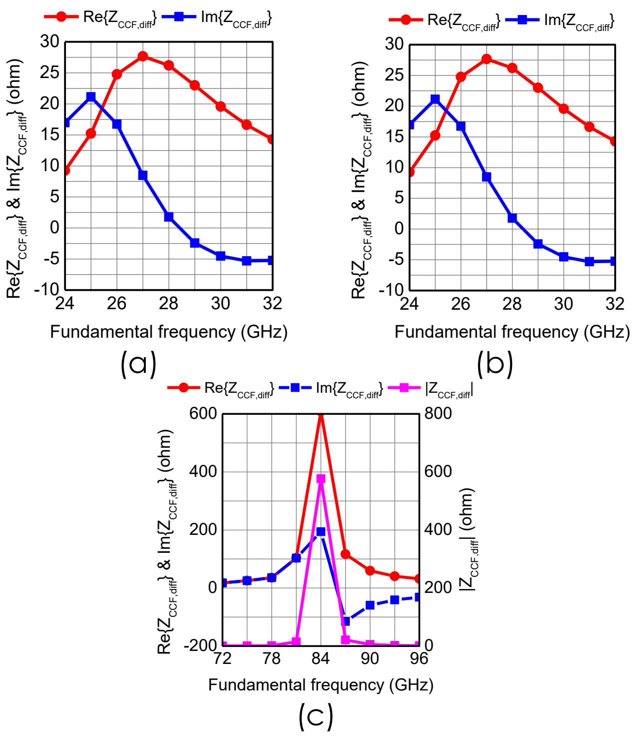

Fig. 3. Frequency response of Re{ZCCF}, Im{ZCCF}, and |ZCCF| at (a) f_o, (b) $2f_o$, and (c) $3f_o$.

(Continued on page 3)

Technology *(Continued from page 2)*

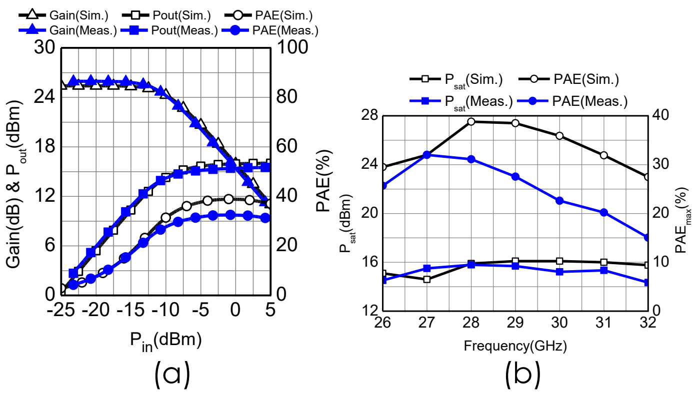

Fig. 4. (a) Gain, output power, and PAE versus P_{in} at 27GHz, and (b) P_{sat} and peak PAE versus frequency.

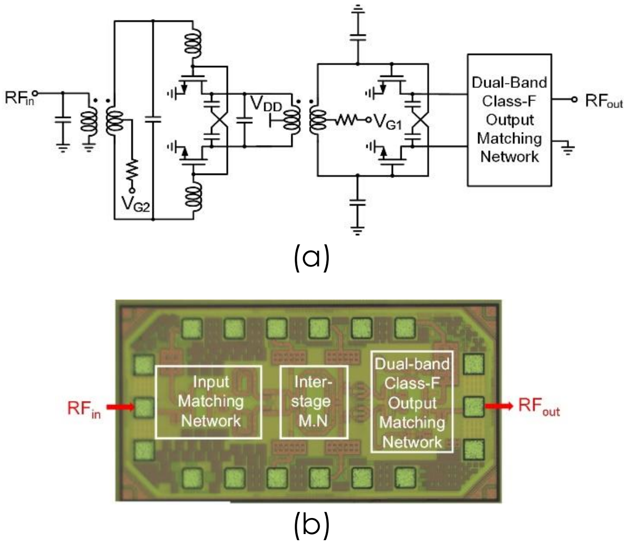

Fig. 5. (a) Schematic, and (b) chip photo of the dual-band class-F PA.

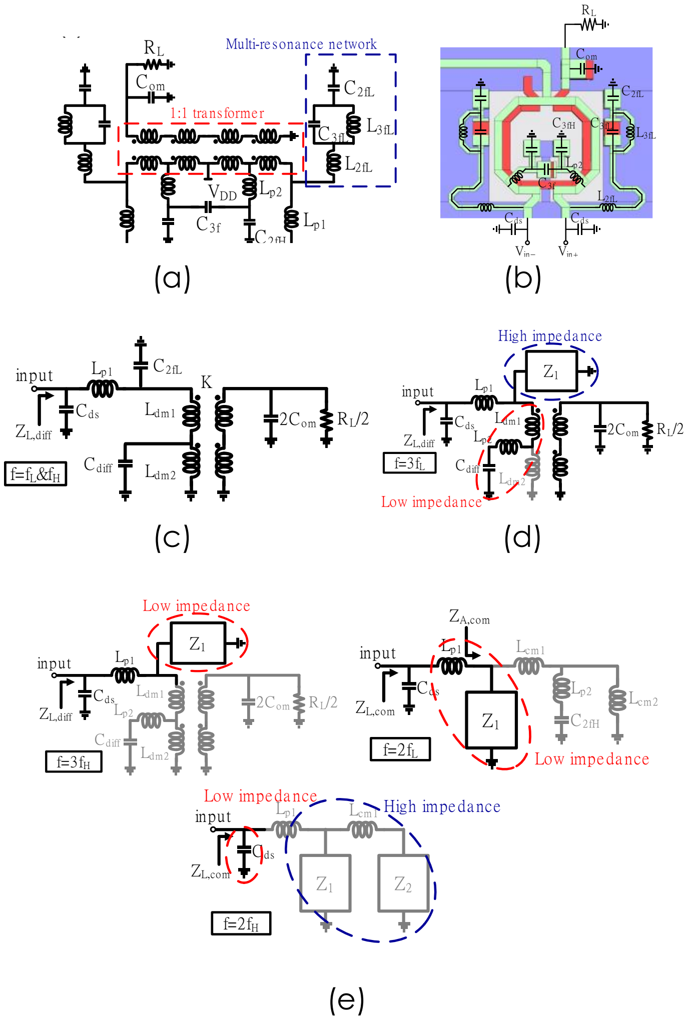

Fig. 6. (a) Detail schematic, (b) layout of the proposed dual-band output matching network, and its equivalent circuits at (c) fundamental, (d) $3f_L$, (e) $3f_H$, (f) $2f_L$, (g) $2f_H$.

Fig. 4(a) shows the simulated and measured gain, output power, and PAE at 27 GHz. The PA achieves the gain of 26 dB, peak PAE of 32%, P_{sat} of 15.5 dBm, and OP_{1dB} of 13.7 dBm. The PAE at the OP_{1dB} is 25.7%. The simulated and measured P_{sat} and peak PAE from 26 GHz to 32 GHz are presented in Fig. 4(b). The 1-dB bandwidth of P_{sat} is from 27 to 31 GHz, and the peak PAE is higher than 20% from 26 to 31 GHz.

CMOS Dual-Band class-F PA [3]

Fig. 5 shows the schematic and chip photo of the 2-stage dual-band class-F PA. The class-AB driver stage is optimized for small-signal gain, while the power stage is biased close to the class-B region to minimize the gap between P_{sat} and OP_{1dB}. In the design of class-F PA, the drain-source parasitic capacitance (C_{ds}) is extracted and considered in the output matching network. Fig. 6(a) and (b) show the schematic and layout of the dual-band class-F output matching network, respectively. The proposed dual-band class-F output matching network is composed of a 1:1 transformer, parallel multi-resonance network (L_{2fL}, C_{2fL}, L_{3fL}, and C_{3fL}), passive components (C_{2fH}, C_{3f}, and C_{om}), parasitic capacitance (C_{ds}), and parasitic inductance of path (L_{p1} and L_{p2}) to realize the multi-resonance network. For the multi-resonance network shown in Fig. 2(a), the L_{3fL}-C_{3fL} tank is designed to resonate at the $3f_L$. The L_{3fL}-C_{3fL} tank behaves like an inductor at a frequency lower than $3f_L$, and it can be combined with L_{2fL} and C_{2fL} to form a series resonator at the frequency which is a little higher than the $2f_L$. Therefore, the multi-resonance network could be regarded as capacitive at $2f_L$. At $3f_H$, the L_{3fL}-C_{3fL} tank is capacitive and can be combined with L_{2fL} and C_{2fL} to form a series resonator and provide a low impedance at $3f_H$.

At f_L and f_H, the L_{p2} is designed to be a small inductor. Hence, the series L_{p2}-C_{diff} behaves like C_{diff}, representing the sum of differential mode half circuit capacitances, C_{3f} and C_{2fH}, and the multi-resonance network is equivalent to a capacitor. Thus, the dual-band class-F output matching network can be converted to a simplified circuit, as shown in Fig. 6(c). Here, both L_{dm1} and L_{dm2} represent

(Continued on page 4)

Technology *(Continued from page 3)*

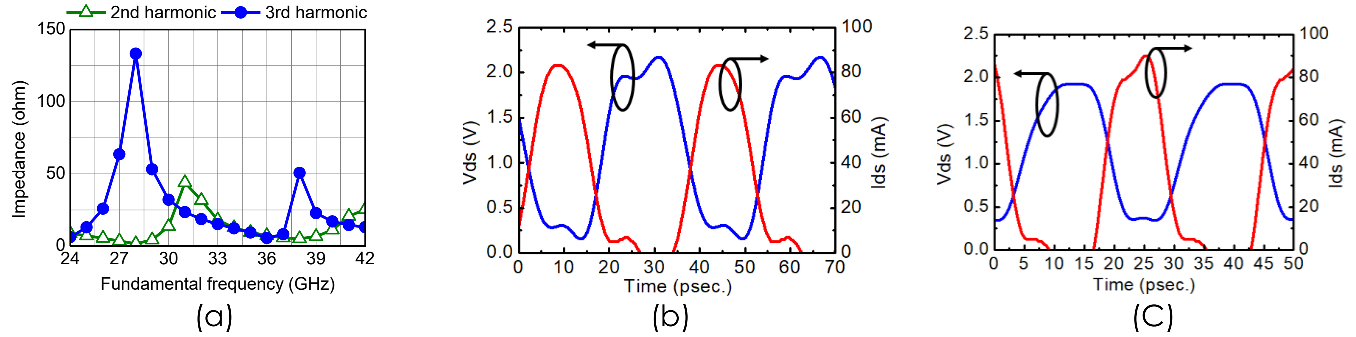

Fig. 7. (a) Simulated harmonic impedance of the proposed dual-band class-F output network, and simulated drain voltage and current waveforms of output transistor at (a) 28 GHz with Pin = -2 dBm and (b) 38 GHz with Pin = 0 dBm.

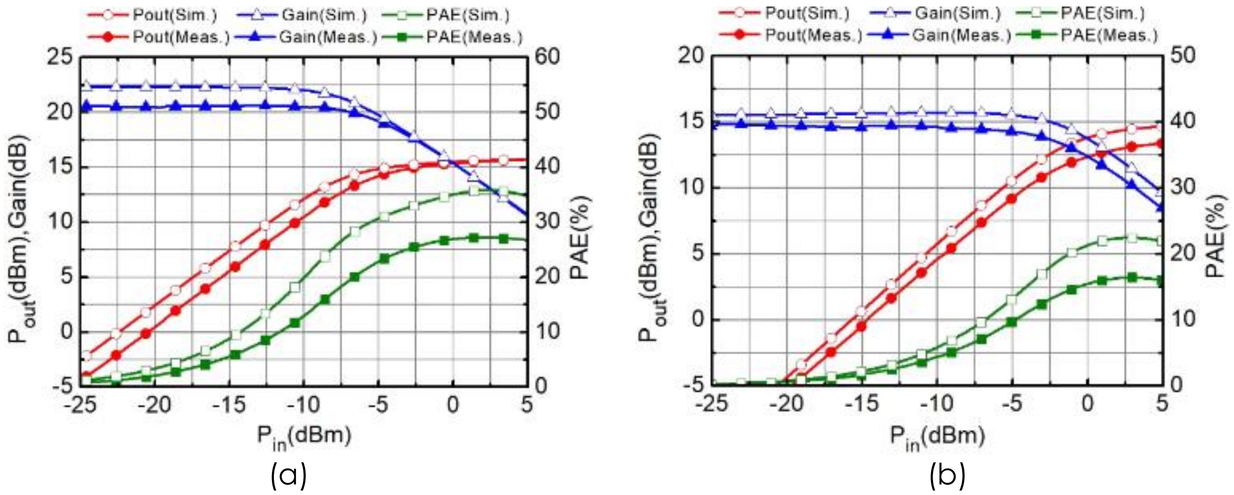

Fig. 8. Large-signal performance versus Pin at (a) 28GHz, and (b) 38 GHz.

the differential mode half circuit inductances of the transformer. This simplified circuit can provide the desired optimal impedance for the PA operating at maximum output power.

At $3f_L$, the impedance of the multi-resonance network (Z_1) is high, and the series resonator consists of L_{dm1}-L_{p2}-C_{diff}, which equivalently contributes a low inductance shown in Fig. 6(d). Therefore, the input impedance, $Z_{L,diff}$, is high due to the parallel resonator consisting of C_{ds} and L_{p1} with inductive path series connected to the ground. Besides, Z_1 becomes a low impedance at $3f_H$, as shown in Fig. 6(e). Thus, $Z_{L,diff}$ is also a high impedance due to the parallel resonator consisting of L_{p1} and C_{ds}.

At $2f_L$, Z_1 exhibits a small negative reactance, which makes $Z_{A,com}$ being dominated by Z_1, as shown in Fig. 6(f). The multi-resonance network and L_{p1} form a series resonator, which provides a low impedance. Therefore, the effect of C_{ds} can be neglected, and $Z_{L,com}$ is a low impedance. Fig. 6(g) shows a simplified half circuit at $2f_H$. Moreover, Z1 becomes a high impedance because $2f_H$ (76 GHz) is close to $3f_L$ (84 GHz), and the Z_2 provides a high impedance. Therefore, $Z_{L,com}$ is dominated by the low impedance of C_{ds}.

Fig. 7(a) shows the simulated harmonic impedances of the proposed dual-band class-F output network. Low second harmonic and high third harmonic impedances are achieved for both 28 GHz and 38 GHz. The simulated voltage and current swings at the drain of the output transistors for both bands are plotted in Fig. 7(b) and (c), which clearly exhibit the class-F function. Fig. 8 shows the simulated and measured gain, output power, and PAE at 28 GHz and 38 GHz. At 28 GHz, the PA achieves the peak PAE of 27.2%, P_{sat} of 15.5 dBm, and OP_{1dB} of 13.9 dBm. The PAE at the OP_{1dB} (PAE_{1dB}) is 21.9%. At 38 GHz, the peak PAE, P_{sat}, OP_{1dB}, and PAE_{1dB} are 16.4%, 13.1 dBm, 11.4 dBm, and 13.8%, respectively.

References

[1] S. Y. Mortazavi, and K.-J. Koh, "Integrated inverse class-F silicon power amplifiers for high power efficiency at microwave and mm-Wave" IEEE J. Solid-State Circuits, vol. 51, no. 10, pp. 2420-2434, Oct. 2016.

[2] Z.-J. Huang, B.-W. Huang, K.-Y. Kao, and K.-Y. Lin, "A high-gain continuous class-F power amplifier in 90-nm CMOS for 5G communication," in 2019 Asia-Pacific Microwave Conference Technical Digest, Singapore, 2019, pp. 177-179.

[3] Z.-J. Huang, Z.-H. Fu, B.-W. Huang, Y.-T. Lin, K.-Y. Kao, and K.-Y. Lin, "A millimeter-wave dual-band class-F power amplifier in 90 nm CMOS," 2020 IEEE International Symposium on Radio-Frequency Integration Technology (RFIT), Hiroshima, Japan, 2020, pp. 70-72.

For more information please contact:
Professor: Kun-You Lin
Email: kunyou@ntu.edu.tw

Technology

Intelligence at the Edge: New Computing Paradigm for IoT and 5G

From Communication and Signal Processing Group

INTRODUCTION

With the rapid development of Internet-of-Things (IoT) and 5G communications in recent years, a paradigm shift, from centralized cloud computing to distributed computing at the edge (or called "edge/fog computing"), is emerging. This new paradigm drives data processing, network control, and storage closer to the network edge, enabling computation-intensive and latency-critical applications on resource-limited mobile devices. Thanks to recent advances in artificial intelligence (AI), many AI methods have been adopted as key enablers to new applications and potential solutions to realizing this new paradigm. The promised gains from AI have inspired extensive research efforts in both academia and industry. As one of the pioneering research teams in edge intelligence, we have proposed the architecture of fog RANs (F-RANs) as shown in Figure 1, which brings the efficient computing capability of the cloud to the edge (e.g., base station, small cell) of mobile network [1]. Based on the architecture, we further study the two research topics: "Flexible Service Platform at the Edge" and "Privacy-Preserving Edge AI Learning."

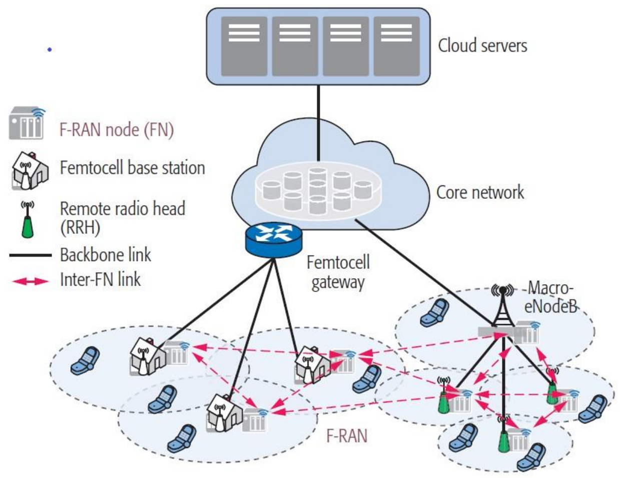

Fig.1 FRAN Architecture.

Flexible Service Platform at the Edge [2] [3]

One burden of realizing edge computing is that the existing network architecture relies on proprietary appliances where software is tightly coupled with specific hardware, and network functions or services are installed and configured manually along with their dedicated devices or boxes. In light of the need for an effective edge computing platform for emerging IoT applications, we propose designing the virtual local-hub (VLH) framework. The framework adopts the microservice concept along with the technology of NFV. We advocate enabling remote function module sharing for increasing the serving capacity and better resource utilization of the edge networks. We develop a testbed for performance evaluation under real-world scenarios. The experiments demonstrate the practicability of the VLH framework in the real world

Privacy-Preserving Edge AI Learning [4]

Edge learning is needed for IoT applications due to privacy concerns and bandwidth limitations. We propose an edge learning system combining semi-supervised learning and federated learning. We identify two challenges for the system: the issues of object size and non-IID data. For the issue that the targeted object may be too small, and improved semi-supervised learning method called OmniLabel is proposed to improve learning performance. Then, consider that data from end devices may be non-IID, which has a negative impact on the learning performance. We propose FedSwap, a new operation that replaces partial federated learning operations based on a few shared data during federated training to alleviate the adverse impact of weight divergence. The performance evaluation on both well-known image dataset and real-world video data confirms the efficacy of OmniLabel and FedSwap.

References

[1] Shih, Y.-Y., Chung, W.-H., Pang, A.-C., Chiu, T.-C., and Wei, H.-Y., "Enabling Low-Latency Applications in Fog-Radio Access Network," IEEE Network, 31(1): 52-58, 2017.

[2] Lin, H.-P., Shih, Y.-Y., Pang, A.-C., and Chou, C.-T., "Virtual Local-hub: A Service Platform on the Edge of Networks for Wearable Devices," IEEE Network, 32(4): 114-121, 2018.

[3] Shih, Y.-Y., Lin, H.-P., Pang, A.-C., Chuang, C.-C., and Chou, C.-T., "An NFV-based Service Framework for IoT Applications in Edge Computing Environments," IEEE Transactions on Network and Service Management, 16(4): 1419-1434, 2019.

For more information please contact:
Professor: Ai-Chun Pang
Email: acpang@csie.ntu.edu.tw

Activities

The 2021 2nd Semiannual Report of Taiwan Electromagnetic Industry-Academia Consortium: Terahertz Technology and Electromagnetic Applications of Macro Models

A full-day workshop of Terahertz technology and Electromagnetic Applications of Macro Models was held on September 2, 2021. Terahertz technology is increasingly used in electromagnetic imaging, and the macro model technology also receives remarkable attention in terms of packaging and multi-network simulation. Industry leaders were invited to share practical experience and unique views, and scholars and experts were invited to serve as moderators to communicate with the speakers. The workshop was conducted online considering the COVID-19 pandemic.

The workshop was hosted by Associate Dean Tzong-Lin Wu and Professor Chun-Hsing Li in the morning and afternoon sessions respectively. At the opening, Professor Ruey-Beei Wu, Chairman of TEMIAC welcomed the attendees to the workshop. More than 170 persons attended the workshop, including researchers from industry, academia, and government.

In the workshop, five presentations were delivered and listed as follows:

1. "Introduction to Macromodeling: Algorithms and Applications ", delivered by the speaker: Professor, Chiu-Chih Chou the Department of Electrical Engineering, National Central University.

2. "Now You See – Super Sensing and Beyond ", delivered by the speaker: Professor Shang-Hua Yang the Department of Electrical Engineering National Tsing Hua University.

3. "The Development of Megahertz Wave Detection Technology in Industrial Applications", delivered by the speaker: Yu-Tai Li the Industrial Technology Research Institute.

4. "Terahertz Filters and Antennas", delivered by speaker: Professor Yu-Hsiang Cheng the Department of Electrical Engineering, National Taiwan University.

5. " CMOS Millimeter-Wave Transceivers and Signal Sources ", delivered by the speaker: Professor Yi-Chun Liu the Department of Electrical Engineering, National Tsing Hua University.

(Continued on page 6)

Fig. 1. Professor Ruey-Beei Wu, Department of Electrical Engineering, National Taiwan University

Fig. 2. Professor Chiu-Chih Chou, Department of Electrical Engineering, National Central University: Introduction to Macromodeling: Algorithms and Applications

Fig. 3. Professor Shang-Hua Yang, Department of Electrical Engineering National Tsing Hua University: Now You See – Super Sensing and Beyond

Fig. 4. Yu-Tai Li, Industrial Technology Research Institute: The Development of Megahertz Wave Detection Technology in Industrial Applications

Activities *(Continued from page 6)*

They delivered broadly from the business trend, technology development, simulation techniques to many demonstrated cases of the THz technology. Through the discussing on current situation and future prospects, they concluded that the THz technology appears to be everywhere in our daily life and Taiwan shall hold the great opportunity.

Thank you very much for participating in the semi-annual report of the Taiwan Electromagnetic Industry-Academy Alliance. If you are interested in various topics in the future, companies or students can communicate with them and discuss with them. There may be opportunities for cooperation. The Taiwan Electromagnetic Alliance will continue. There will be these special lectures.

Fig. 5. Professor Chien-Nan Kuo, Department of Electronics Engineering, National Yang Ming Chiao Tung University

Fig. 6. Professor Yu-Hsiang Cheng, Department of Electrical Engineering, National Taiwan University: Terahertz Filters and Antennas

Fig. 7 Professor Yi-Chun Liu, Department of Electrical Engineering, National Tsing Hua University: CMOS Millimeter-Wave Transceivers and Signal Sources

Corner of Student News

APPLE Internship Experience

Article by PhD student Sung-Feng Huang

I went to Apple for an internship in Cupertino, California in June last year. I was a master student at the Graduated Institute of Communication Engineering, NTU. I attempted to get the internship because of the recommendation of my senior. This is my first trip to the United States, and also the first time to fly abroad alone and stay abroad for 3 months. I have no companions on this trip, but some of my friends I know are also nearby, so I ate with them the day I arrived and asked them about life in the United States. My housing was arranged at Sunnyvale. The area is very sparsely populated. It would take 20 minutes to walk to the downtown near the station to have a restaurant. If you need a supermarket, there is a Chinese downtown next to the company. These two places are where I mainly purchase food and eat. It is also because of the large area and sparse population, the transportation is not convenient, and the car rental is also quite expensive, so most of the holidays will not go with a companion. In the first half of the internship, I mostly gathered in my rental room with another friend who was an intern at Amazon during my holidays, cooking or chatting in person. Unlike Apple, Amazon has a lot of work, and Apple asks not to work overtime. In the second half of the internship, I visited the Airbnb company with some friends on a holiday. Each room in the company was decorated in the style of Airbnb from all over the world. In addition, I also went to Yosemite in the last week of my internship. In Yosemite, I can see many sources of framing of the macbook desktop, and the air is quite fresh. In addition, I watched a movie with some friends in American cinemas. The first time I watched a movie without subtitles, I found it amazing. The chairs in the cinema are electrically adjustable and very advanced. I am very happy to have this opportunity to go to the United States for an internship to broaden my knowledge and increase life experience. Although it was not a smooth journey, and memories are not all good, it will still be an important journey in my life.

Photo in Cupertino.

National Taiwan University Graduate Institute of Communication Engineering

No.1, Sec.4, Roosevelt Road,
Taipei 10617, Taiwan

Phone
+886-2-3366-3075

Fax
+886-2-2368-3824

E-mail
gicenewsletter@ntu.edu.tw

Visit us at:
http://www.comm.ntu.edu.tw

Editor in Chief
Prof. Shih-Chun Lin
Editor
Yi-Chi Chen